DARLA: Data Assimilation and Remote Sensing for Littoral Applications

Andrew T. Jessup
Chris Chickadel, Gordon Farquharson, Jim Thomson
Applied Physics Laboratory
University of Washington
Seattle, WA 98105
phone: (206) 685-2609 fax: (206) 543-6785 email: jessup@apl.washington.edu

Robert A. Holman
Merrick Haller, Alexander Kuropov, Tuba Ozkan-Haller
Oregon State University
Corvallis, OR 97331
phone: (541) 737-2914 fax: (541) 737-2064 email: holman@coas.oregonstate.edu

Steve Elgar
Britt Raubenheimer
Woods Hole Oceanographic Institution, MS11
Woods Hole, MA 02543
phone: (508) 289-3614 fax: (508) 457-2194 email: elgar@whoi.edu

Award Number: N000141010932

LONG-TERM GOALS

Our long-term goal is to use remote sensing observations to constrain a data assimilation model of wave and circulation dynamics in an area characterized by a river mouth or tidal inlet and surrounding beaches. As a result of this activity, we will improve environmental parameter estimation via remote sensing fusion, determine the success of using remote sensing data to drive DA models, and produce a dynamically consistent representation of the wave, circulation, and bathymetry fields in complex environments.

OBJECTIVES

The objectives are to test the following three hypotheses:

1. Environmental parameter estimation using remote sensing techniques can be significantly improved by fusion of multiple sensor products.
2. Data assimilation models can be adequately constrained (i.e., forced or guided) with environmental parameters derived from remote sensing measurements.
3. Bathymetry on open beaches, river mouths, and at tidal inlets can be inferred from a combination of remotely-sensed parameters and data assimilation models.

Report Documentation Page

Form Approved
OMB No. 0704-0188

1. REPORT DATE	2. REPORT TYPE	3. DATES COVERED
30 SEP 2013		**00-00-2013 to 00-00-2013**

4. TITLE AND SUBTITLE	5a. CONTRACT NUMBER
DARLA: Data Assimilation and Remote Sensing for Littoral Applications	5b. GRANT NUMBER
	5c. PROGRAM ELEMENT NUMBER
6. AUTHOR(S)	5d. PROJECT NUMBER
	5e. TASK NUMBER
	5f. WORK UNIT NUMBER
7. PERFORMING ORGANIZATION NAME(S) AND ADDRESS(ES) **University of Washington,Applied Physics Laboratory,Seattle,WA,98105**	8. PERFORMING ORGANIZATION REPORT NUMBER
9. SPONSORING/MONITORING AGENCY NAME(S) AND ADDRESS(ES)	10. SPONSOR/MONITOR'S ACRONYM(S)
	11. SPONSOR/MONITOR'S REPORT NUMBER(S)

12. DISTRIBUTION/AVAILABILITY STATEMENT
Approved for public release; distribution unlimited

13. SUPPLEMENTARY NOTES

14. ABSTRACT

15. SUBJECT TERMS

16. SECURITY CLASSIFICATION OF:			17. LIMITATION OF ABSTRACT	18. NUMBER OF PAGES	19a. NAME OF RESPONSIBLE PERSON
a. REPORT	b. ABSTRACT	c. THIS PAGE			
unclassified	**unclassified**	**unclassified**	**Same as Report (SAR)**	**25**	

APPROACH

Our overall approach is to conduct a series of field experiments combining remote sensing and in situ measurements to investigate signature physics and to gather data for developing and testing DA models. To ensure early and ongoing testing, we performed a pilot experiment at Duck, NC, using tower-based remote sensing (EO, radar, IR) and current versions of the DA modeling system. We participated in the field experiments in May 2012 at New River Inlet near Camp LeJeune, NC and in May and June of 2013 at the mouth of the Columbia River near Astoria, OR under the ONR-sponsored Inlets and Rivers Mouth Dynamics Departmental Research Initiative (RIVET I and II). This approach benefits both the remote sensing research (by leveraging the RIVET in situ measurements) and RIVET itself via our integrated remote sensing and DA modeling system. We also conducted airborne measurements and in situ measurements at the mouth of the Columbia River for approximately one to two weeks each during July and September 2013. The combined capabilities provide an innovative solution that couples spatially dense sampling with data assimilation methods to study the complicated dynamics of interacting wave, bathymetry, and current fields. The key to this project is an interactive process that blends sophisticated remote sensing, in-situ sensing, and data assimilation modeling. Our approach is to conduct closely coupled field and numerical model experiments to test the hypotheses listed above. Work on each facet informs the work on the others, and conflicts in results or interpretations are resolved by testing the hypotheses and the sensitivity of the results to a range of parameter variations.

WORK COMPLETED AND RESULTS

During the third year, we participated in the RIVET II DRI experiment in May and June 2013 and supplementary airborne and in situ measurements in July and September 2013 at the mouth of the Columbia River. We also worked on analysis and assimilation of the data from the Duck pilot and RIVET I experiments.

Due to the number of investigators involved and the complexity of the project, we have chosen to provide a section for each team which combines their Work Completed and Results contributions. The lettered sections correspond to the following teams:

A. Infrared Remote Sensing and Lidar– UW: Chickadel and Jessup
B. Electro-Optical Remote Sensing – OSU: Holman
C. Microwave Remote Sensing – UW: Farquharson
D. Microwave Remote Sensing – OSU: Haller
E. In situ Measurements – UW: Thomson
F. In situ Measurements – WHOI: Elgar and Raubenheimer
G. Numerical Modeling and Data Assimilation – OSU: Ozkan-Haller and Kurapov

A. INFRARED REMOTE SENSING AND LIDAR - UW

CASIE

In FY13, we added a nadir-pointed lidar to the Compact Airborne System for Imaging the Environment (CASIE). CASIE now consists of the dual-beam along-track interferometric (ATI) synthetic aperture radar (SAR), two infrared cameras, a visible wavelength camera, and the point

measuring lidar. Accurate plane platform positioning and attitude is reported by an inertial navigation system (INS) consisting of a Novatel Propak-V3 GPS and an iMar FSAS inertial motion unit (IMU). Data are recorded at both at 100Hz and 5Hz for radar and imaging application.

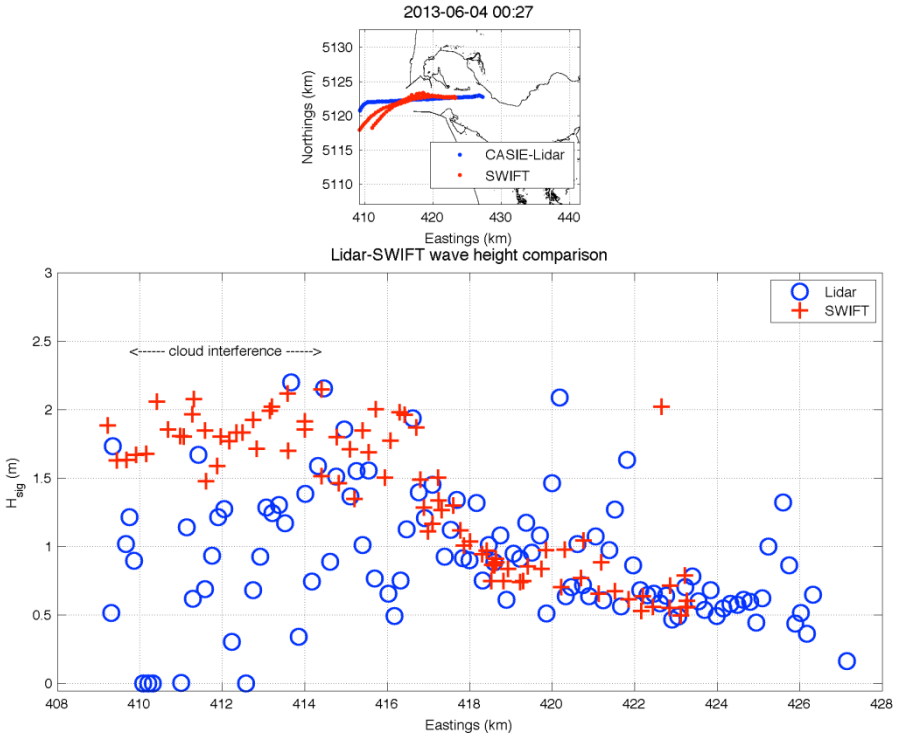

Figure A1. (top) SWIFT and CASIE transects over the MCR on 6 June 2013 during an ebb flood, time is in UTC. (bottom) Wave height reported by the SWIFT and estimated from the Lidar data agree well and show a sharp decease in wave height through the mouth and into the estuary due to wave current interaction. Wave height estimates offshore (west of 416m) are degraded due to intermittent cloud interference.

Lidar

Before the first deployment of the system over the Mouth of the Columbia River in April this year, CASIE was tested over Deception Pass, north of Whidbey Island, and over the Strait of Juan de Fuca for functionality of the lidar unit (a Riegl model LD90-3800EHS-FLP). The lidar is capable of range measurements of up to 750m and at rates up to 12 KHz without quality control or timing information, though we operate it at 3KHz due to ensure accurate timing information is included in the data stream. The lidar was deployed throughout the MCR experiments whenever we flew the aircraft with the intention of demonstrating sea surface elevation and wave height estimation directly from aircraft platforms. Processing included correcting for plane position and first order plane attitude, recorded in the INS data stream. Wave height is estimated by calculation of a running standard deviation filter to estimate the variability spanning several wavelengths. Figure A1 shows an example comparison between the Lidar estimate significant wave height and the significant wave height estimated from a SWIFT drifter on an ebb tide on 6 June 2013 at 1700 PDT. Both measurements show approximately 2m wave heights offshore the mouth that decrease into the estuary due to wave current interaction. Lidar wave heights are partially corrupted due to intermittent in the MCR, west of 416 km easting.

Thermal Imaging

Analysis of thermal imaging during 2013 covered finalizing techniques to estimate wave dissipation, improved mapping of NRI airborne IR data, continued estimation of inlet currents from the NRI imaging tower, and fixed and airborne measurements at the 2013 RIVET II – MCR experiment.

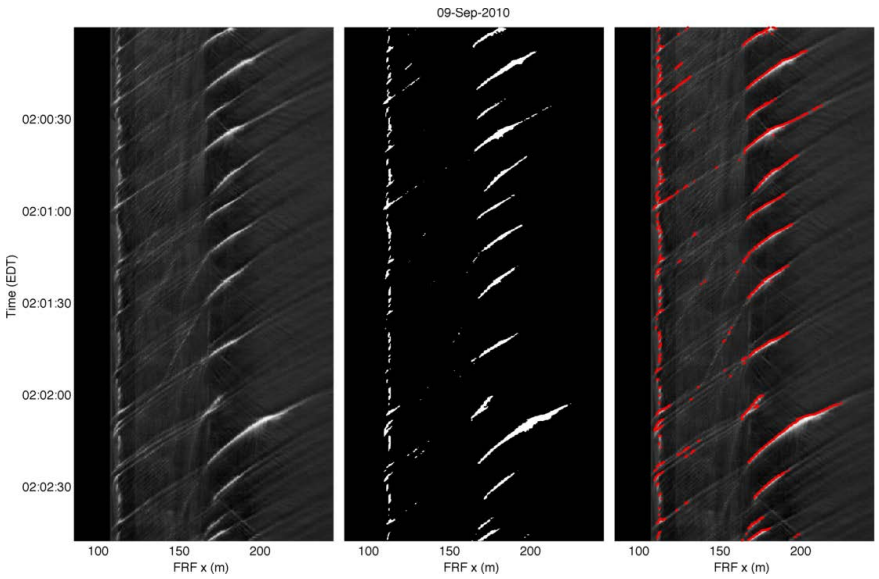

Figure A2. (left) Two-minute thermal image timestack of wave breaking at Duck during SZO. (center) Mask resulting from automated isolation of active breaking. (right) Automated counting, in red, of identified waves.

Wave Dissipation

Using data from the 2010 Surf Zone Optics (SZO) data, master's student Roxanne Carini has been developing a method to both isolate active wave breaking from passive, residual foam and estimate wave dissipation. Breaking waves are visible in the surf zone as brighter (warmer) regions, due to the higher emissivity of sea foam compared with the surrounding undisturbed water. An early conformational finding of this research has been that passive foam has a cooler signature possibly due to enhanced heat flux. Using this a technique was developed to objectively automatically isolate active breaking, which is based on identifying key features of the surface temperature probability distribution function. Once isolated, metrics of active breaking are used to derive remote estimates of wave dissipation through application of either a breaking rate model by *Janssen and Battjes* (2007) or the wave roller model of *Duncan* (1981). Figure A2 shows the results from automated isolation of breaking waves including and their leading edge. Figure A3 reveals the resulting wave count and roller length metrics identified during SZO. Figure A4 shows the comparison of TKE dissipation rate estimated from an in situ current meter profiler (work by Jim Thomson) and IR-dervied estiamtes of wave dissipation. Though the remote sensing methodologies are based on different data metrics, their magnitudes are very similar. Comparisons against the in situ estimates show IR based data are approximately 1-1.5 orders of magnitude larger. IR wave dissipation measures also better correlate with near surface (maximum) estimates and not depth integrated values, which is reasonable if wave dissipation is more confined to the near surface. Analysis of the wave dissipation data is being finalized and aspect of the in situ – remote sensing mismatches are being investigated.

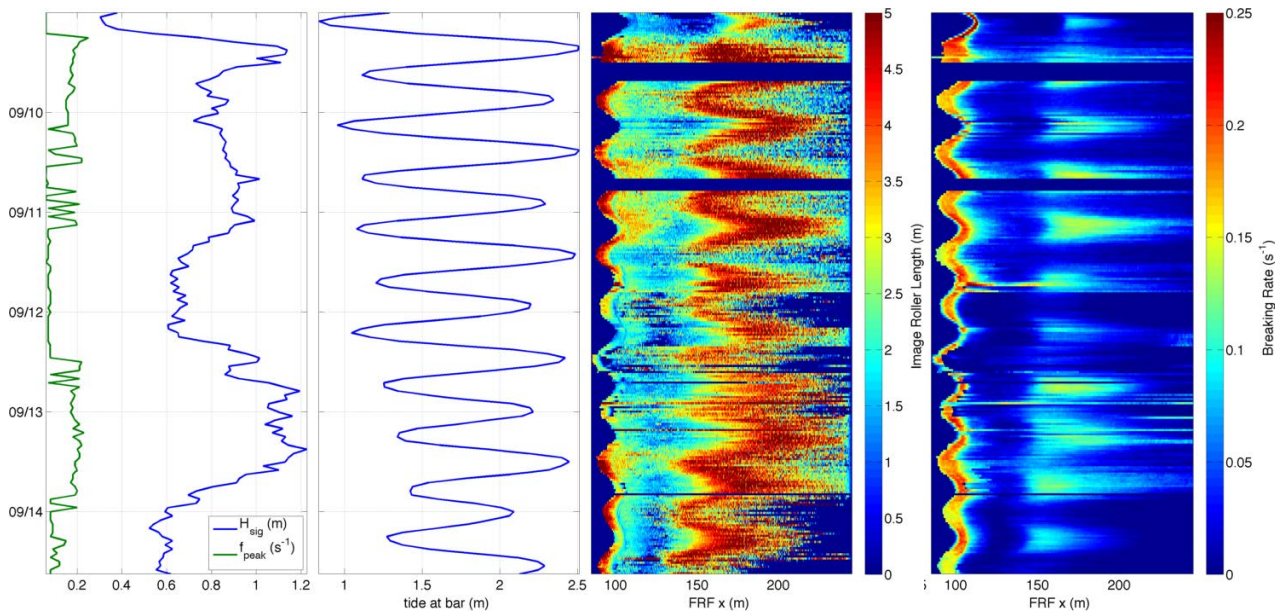

Figure A3. (left) Wave conditions during Surf Zone Optics and (center left) tidal elevation. (center right) Median wave roller length and (right) wave breaking rate during the SZO experiment. Variation of the roller length and breaking rate corresponds primarily to tidal modulation of the water depth, but periods of larger storm waves can also be seen near September 11 and 13.

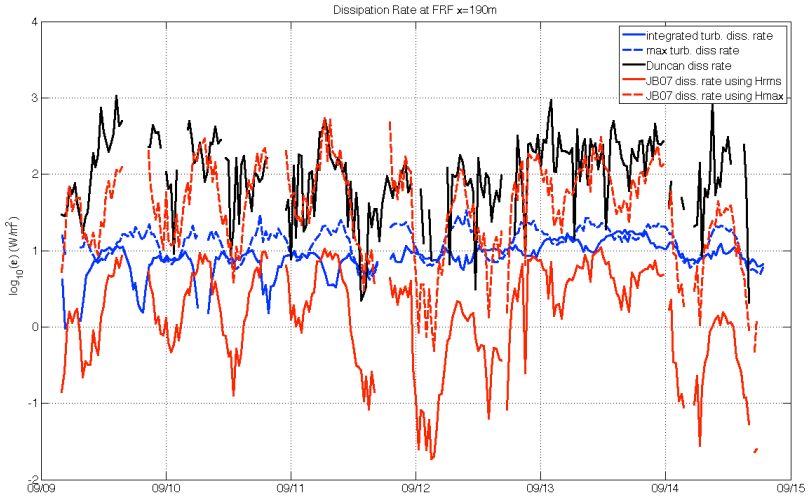

Figure A4. In situ TKE dissipation rates (provided by Jim Thomson) compared against IR-derived wave dissipation rates at location near the bar crest, x = 190m. Tidal modulation in dissipation is evident in all the estimates and the in situ estimates are approximate 1-1.5 orders of magnitude lower than the IR-based estimates.

CASIE New River Inlet plume

Airborne thermal mapping of the New River Inlet has been improved and preliminary comparisons with available in situ data are underway. Figure A5 shows an example ebb plume temperature structure overlain with velocity and near-surface temperature data collected from the SWIFT drifters (via Jim Thomson) near the same time as the image was recorded. Typical features of the plume

include multiple internal temperature fronts and preferred plume location lobes due to distinct channels in the ebb tidal delta. IR temperature observations of warm water ejected at the ebb jet locations into colder ocean water are support by SWIFT observations which show 1C - 0.5C difference between plume water and ocean water. Though not shown we have also documented the strong wind dependence on plume location and direction, and in this example offshore winds are guiding the plume away from shore.

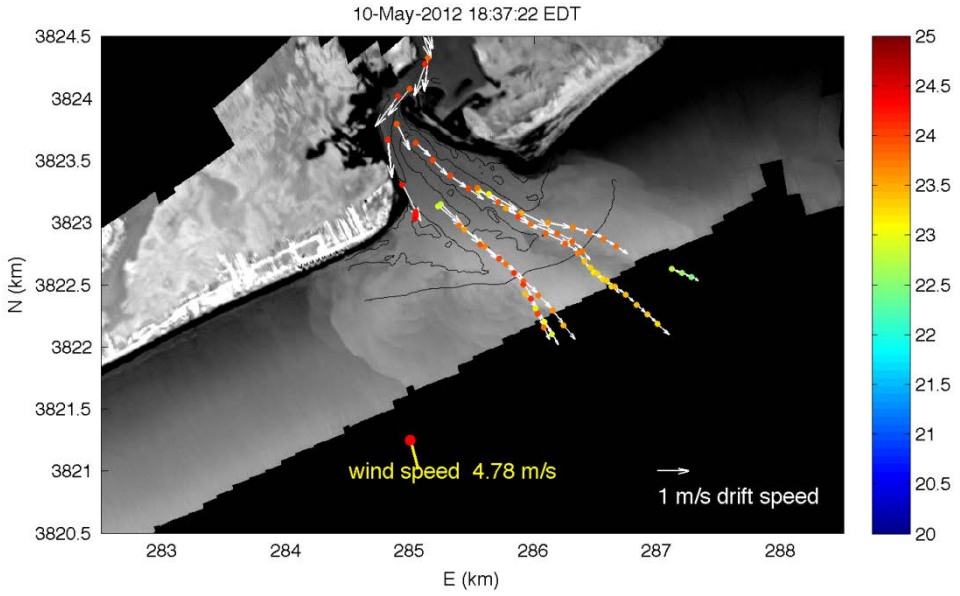

Figure A5. CASIE IR plume map of New River Inlet reveals the warm plume water exiting the inlet through channels in the ebb delta. SWIFT drifter temperature and surface velocity support the inferred surface temperature and flow patterns.

New River Inlet Circulation

Using IR data from the NRI imaging tower we have computed surface velocities from the available record (approximately 2.5 weeks of near continuous IR imagery) using a 2D PIV algorithm. This data will be used to help drive data assimilation models of the inlet flow and bathymetry. Our results to date indicate that the PIV algorithm is sensitive to thermal contrast as indicated but the plots in figure A6. We find that in comparison to in situ velocity measurements (provided by Britt Raubenheimer and Steve Elgar) our IR-derived surface currents will tend to zero velocity during daylight hours, presumably when solar heating homogenizes surface temperatures. To try to improve the velocity measurements we are testing a previously developed algorithm (*Chickadel et al*., 2003) to estimate longshore currents in the surfzone. The increased robustness of the method comes at the cost of only being able to estimate only along-channel currents.

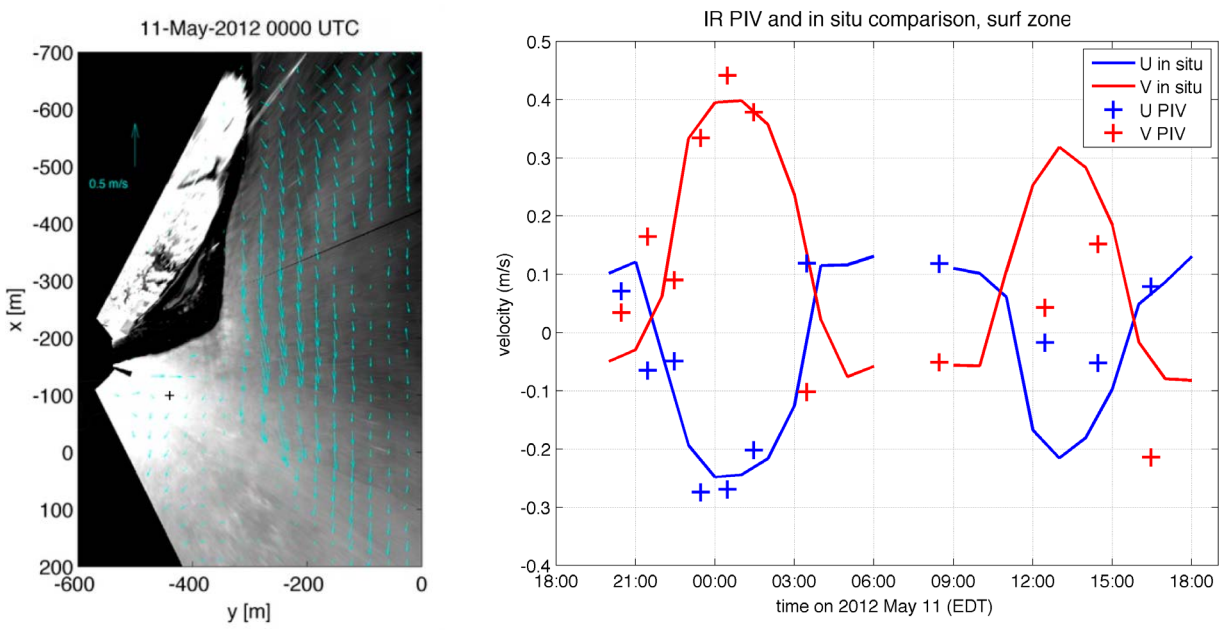

Figure A6. (left) 2D PIV currents on an ebb tide during RIVET I - NRI. The '+' indicates location of an in situ current meter (WHOI) used for validation. (right) Comparison of the along and cross-shore PIV and in situ current measurements shows the best agreement during noght hours when temperature contrast is strongest.

Columbia River Mouth

Much of the newest work performed this year has been focused on sampling for the second field experiment at the Mouth of the Columbia River (MCR). IR data was recorded from both a fixed location on the Cape Disappointment lighthouse on the north side of the inlet, integrated into the Argus station installed there in March 2013, and from focus and monthly CASIE flights from April until September. Lighthouse data were designed to capture both waves and fronts formed there. Analysis of this data will begin in FY14.

Airborne IR (CASIE) data is intended to provide synoptic data of water masses, fronts and mixing revealed through temperature variation at the surface. An example was recorded on a flight on June 3rd during the ebb current, where significant surface temperature features were observed at the mouth south of the north jetty. Figure A7 details the strong surface mixing in this region, which probably linked to detachment of the river/estuary water from the bed as it flows into the ocean at the mouth, called liftoff. The surface temperature is marked by flow parallel streaks with order 100m spacing and character that varies across the inlet. Interesting the origination of these features suggest a linear and continuous initiation point. In this example, a Remus vehicle (operated by Craig McNeil - APL) was also flown simultaneously through the inlet and recorded vertical profiles of temperature and other parameters. The location of thinning of the surface warm layer shows good agreement with the temperature feature in the IR data. Future analysis will focus on mapping the temporal and spatial evolution of the surface mixing noting scales of the streaks and boils and strength of the temperature contrast with stage of the ebb flow.

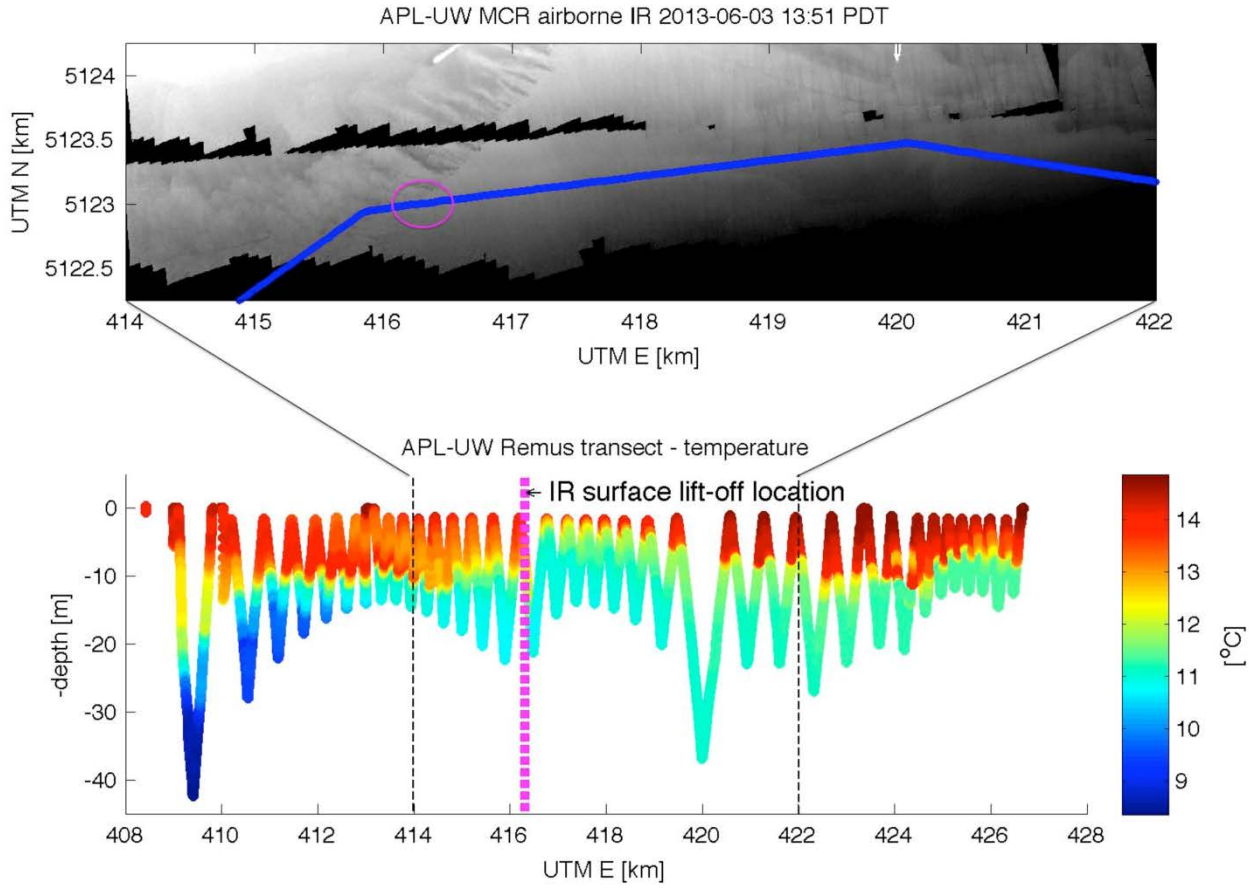

Figure A7. (top) Thermal image mosaic recorded from CASIE during an ebb current. Linear mixing features near east = 415-416km is likely due to liftoff processes at the mouth. (b) Temperature profiles recorded from a Remus vehicle (Craig McNeil - APL) detail thinning of the surface warm layer at this location and thickening of the warm layer offshore of the liftoff due to strong mixing and entrainment of the ocean water from below.

B. ELECTRO-OPTICAL REMOTE SENSING - OSU

The goal of the electro-optical component of DARLA is to develop and test algorithms for estimating relevant geophysical variables based on electro-optical (EO) data, to work with modelers who will be developing methods to assimilate these data using appropriate statistical methods of data assimilation, and to compare data to synchronous results from companion radar and infrared sensors to search for new opportunities in data fusion. Field tests have been key to developing our understanding and methods and have included the two-week Surf Zone Optics experiment at Duck, NC in September, 2010, a three-week field experiment in the unjettied New River Inlet in May, 2012 and a roughly five-week experiment at the Mouth of the Columbia River (MCR) in May-June, 2013. The electro-optical component of the recent MCR work started shortly before in-situ sampling but will actually continue for one full year in order to capture a full annual signal of river and ocean conditions. Time series data

from optical collections have been made available on a common ftp site in MATLAB format for all other investigators.

Our efforts to develop and test algorithms to estimate geophysical variables from EO signals have followed several directions. The most robust result produced thus far under this grant has been the cBathy algorithm for the robust estimation of frequency-wavenumber-direction triads and the bathymetry that is derivable from that data [*Holman et al.*, 2013]. For open beach conditions like Duck, NC, this algorithm has shown bias and rms errors of 0.19 and 0.51 m, respectively over a 0.5 km^2 test region sampled over 16 monthly surveys. The algorithm has recently been tested by colleagues under high frequency wave conditions of the North Sea where performance should be worse but has been found to perform remarkably well (Figure B1). We are now testing the modifications needed to operate under combined wave-current conditions of tidal inlets using the data returned from the two most recent experiments with the goal of estimating depth and currents simultaneously.

Our second main theme is the testing of methods for the remote estimation of incident wave dissipation from EO observations of wave breaking, a strong signal in all remote-sensing modalities. The spatial and temporal distribution of dissipation directly determines the forcing of low-frequency flows and currents, so the assimilation of such data into a modeling system would be powerful.

Jointly with Merrick Haller, we have published a state of the art summary of all aspects of the nearshore remote sensing problem in the Annual Reviews of Marine Science [*Holman and Haller*, 2012]. This describes a superset of the DARLA research program including future directions.

The cBathy paper has now been published [*Holman et al.*, 2013]. The algorithm, including a user manual, has been made available to many collaborators and is being tested under a wide variety of wave and beach conditions. As shown in Figure B1, the results seem surprisingly good.

On May 2, 2013, we installed a new Argus Station at Cape Disappointment in time for the RIVET II field experiment. This will run for one year to capture the full seasonal variations of river and ocean conditions. The large scales of the MCR have forced a sampling scheme in which several cameras have no visible control points. Thus we have been forced to develop a new method of inter-camera alignment.

Our primary result has been the development of robust algorithms for the estimation of wave variables and bathymetry under a wide variety of conditions and in the face of large variations in data quality including fog and rain. The method is now being tested around the world. Estimated confidence limits allow these results to integrated into data assimilative tools or other downstream products.

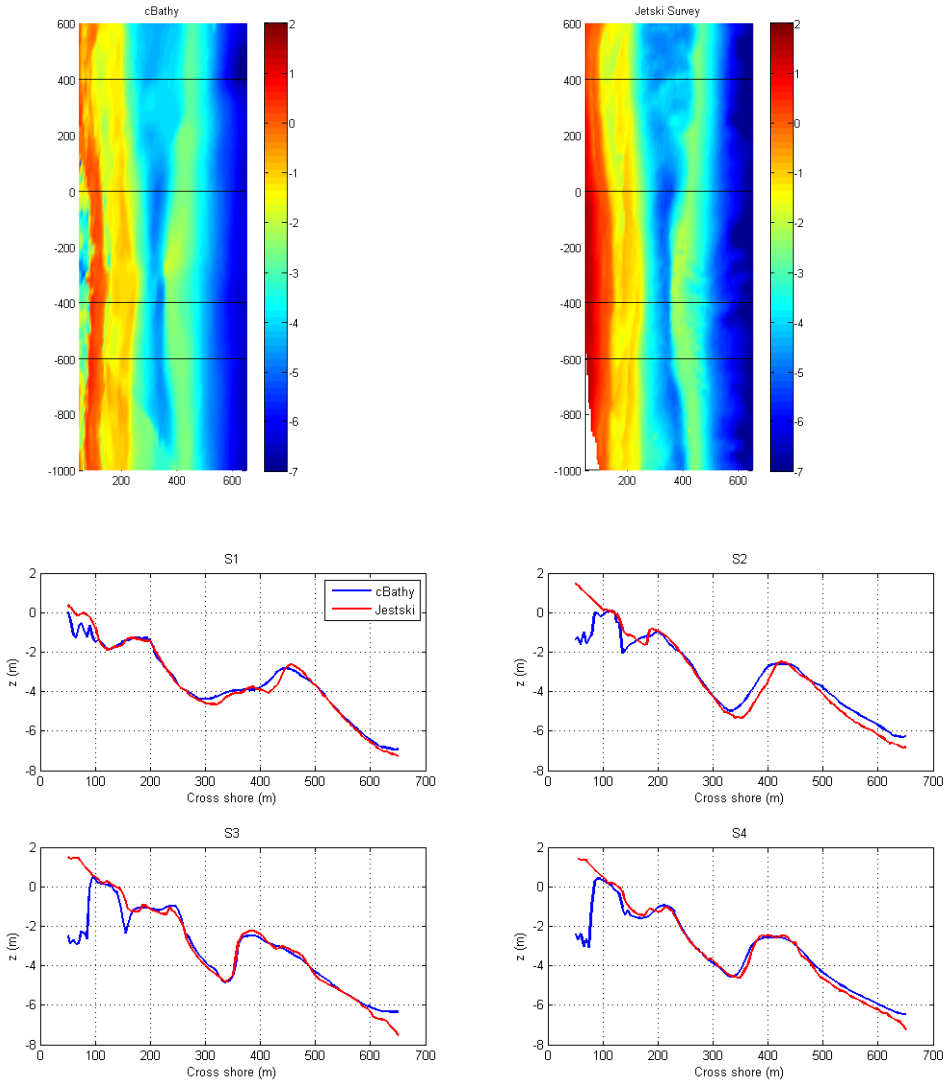

Figure B1. The upper panel shows a cBathy bathymetry estimate (left) compared to ground truth bathymetry (right) for an example data set from Egmond, The Netherlands. The lower panel shows four data slices (marked by black lines in the upper panel). Results are better than expected, given the short wave periods of the North Sea. (Analysis by Leo Sembiring, Deltares).

C. MICROWAVE REMOTE SENSING - UW

Synthetic Aperture Radar

In FY13, we focused on improving the processing for the New River Inlet (NRI) data to retrieve surface current estimates, and on making measurements over the mouth of the Columbia River.

microASAR Calibration

We continue to refine the data quality from the synthetic aperture radar. While, frequency-modulated continuous wave (FMCW) radars are appealing for implementing airborne synthetic aperture radars (SAR), careful calibration of the phase response of the radar is required. This calibration is necessary

because receiver beat frequency in an FMCW radar is equivalent to distance from the radar, so phase differences between receiver channels introduce a range dependent phase offset in the interferograms. We have developed a lab-based calibration scheme that reproduces the range-dependent phase ripple seen in the ATI interferograms (Figure C1, left), and allows us to almost completely remove the range-dependent phase ripple (Figure C1, right). This work was presented at the 2013 International Geoscience and Remote Sensing Symposium in Melbourne, Australia. We are now working on improving the robustness of the calibration technique.

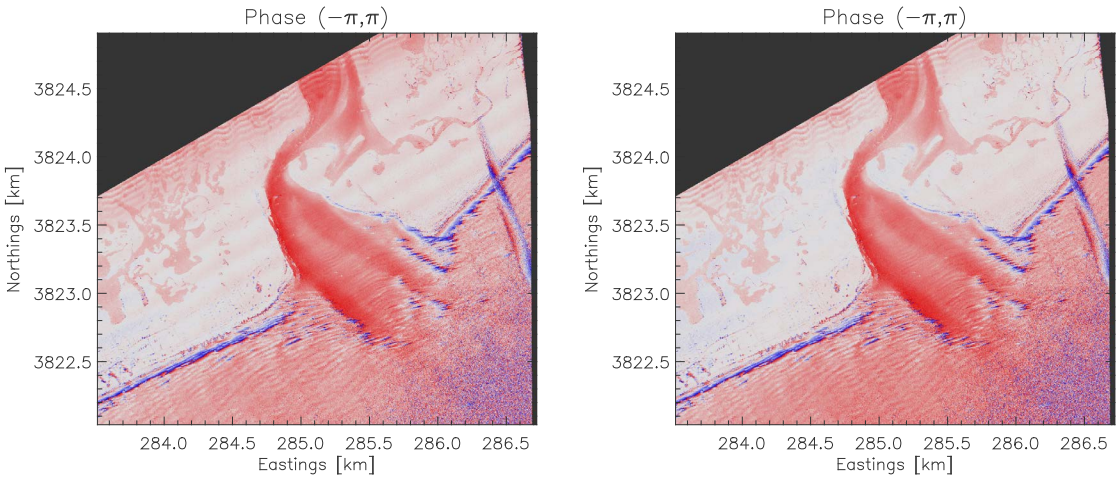

Figure C1: Interferometric phase without phase calibration (left) and with phase calibration (right). The range-dependent phase ripple has been almost completely eliminated.

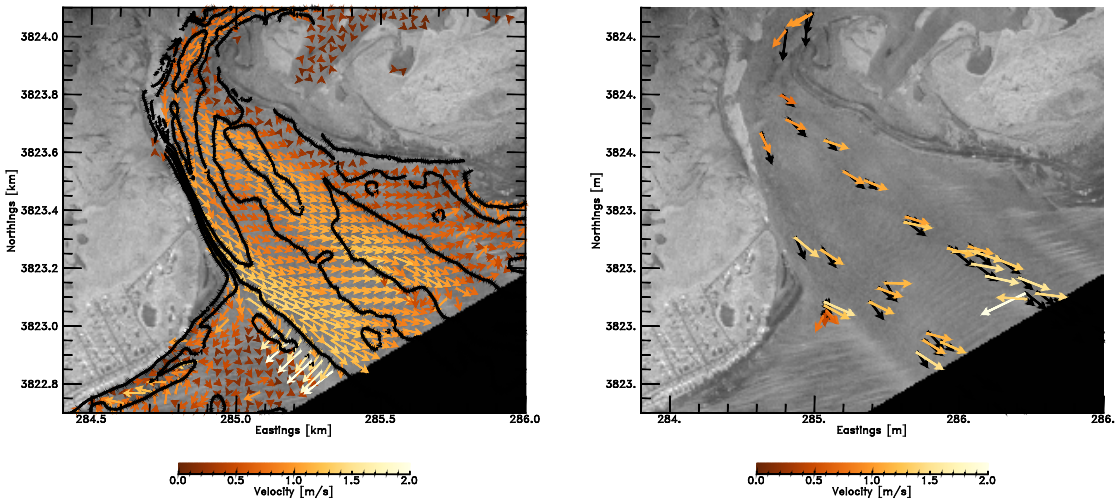

Figure C2: Left: ATI SAR surface velocity field during max ebb at the New River Inlet (data acquired on May 10, 2012 between 21:58:40 and 22:01:36 UTC). Right: Comparison of ATI SAR velocity (color) and SWIFT drifter velocity (black). The SWIFT data was collected between 21:00 UTC and 23:00 UTC.

Velocity Field Retrieval
We have continued to develop our surface velocity retrieval code for the microASAR data. Our code now uses meteorological data to remove Doppler shift due to the Bragg resonant waves from ATI SAR data. An example surface velocity field in Figure C2 (left).

We are using SWIFT drift velocity data (Jim Thomson, APL-UW) to validate our surface current estimates (Figure C2, right). ATI SAR velocity magnitude compares very well with the SWIFT surface current estimates, but the direction of the radar-derived velocities have an eastward bias, especially in the mouth, where wave effects may be important.

Nearshore Wave Height Retrieval
We have developed a technique to estimate nearshore ocean breaking wave height from our ATI SAR data. The technique exploits the azimuthal shift induced by moving scatterers in SAR imagery. Specifically, moving scatterers are shifted azimuthally by a displacement that is equal to the velocity of the scatterer. It is expected that a nearshore breaking wave will have multiple scatterers that move with different velocities. We find that length of the azimuthal streaks are correlated with breaking wave height (correlation coefficient is 0.78) for a range of wave conditions (Figure C3). Red circles correspond to situation when wave propagation direction was roughly orthogonal to shoreline (the angle of waves arrival was 70° to 110°). Blue stars and black rectangles correspond to slightly oblique wave angles of 110° to 140° and 40° to 70° respectively. The angle of wave arrival does not appear to significantly affect the retrieval of wave height in the range 30 to 70 cm. Pressure sensor data from Steve Elgar and Britt Raubenheimer (WHOI) were used in this comparison.

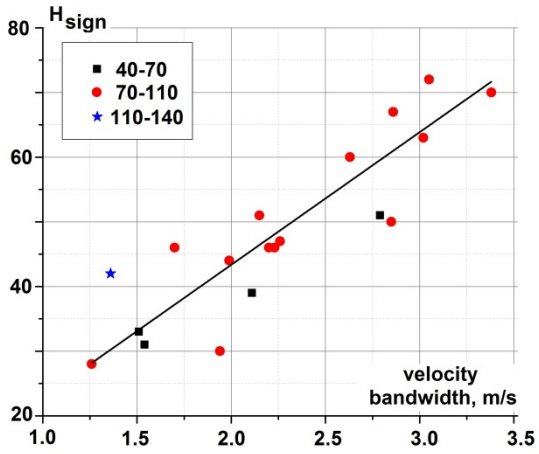

Figure C3: Relationship between ATI SAR breaking wave signature length (proportional to the range of velocities in the breaking wave), and breaking wave amplitude.

The scatter diagram, presented in Figure C3, can be fitted linearly:

$$H_{sign} = 20.5 \times \Delta V_r + 2.33$$

where H_{sign} is the wave height (cm), ΔV_r is the radial velocity bandwidth of breaking waves (m/s). This work was presented at the 2013 International Geoscience and Remote Sensing Symposium in Melbourne, Australia.

MCR Field Measurements and Analysis

We performed measurements with CASIE in April, May/June, July, and September over the Mouth of the Columbia River. In total, we collected data on 31 days in this period (April: 4 days; May/June: 15 days; July: 5 days; September: 4 days).

We have started processing the microASAR data from the MCR experiments. For efficient processing and analysis, we have divided the domain into four areas of interest (Figure C4). This method allows us to process the SAR data efficiently because we can form SAR images only in the areas of interest, which reduces processing time.

Figure C4: Zones of the MCR in which ATI SAR data analysis will be focused. The top-left zone includes the area around the North Jetty, the top-right zone includes Jetty A, and the bottom-right zone includes the South Jetty and Clatsop Spit.

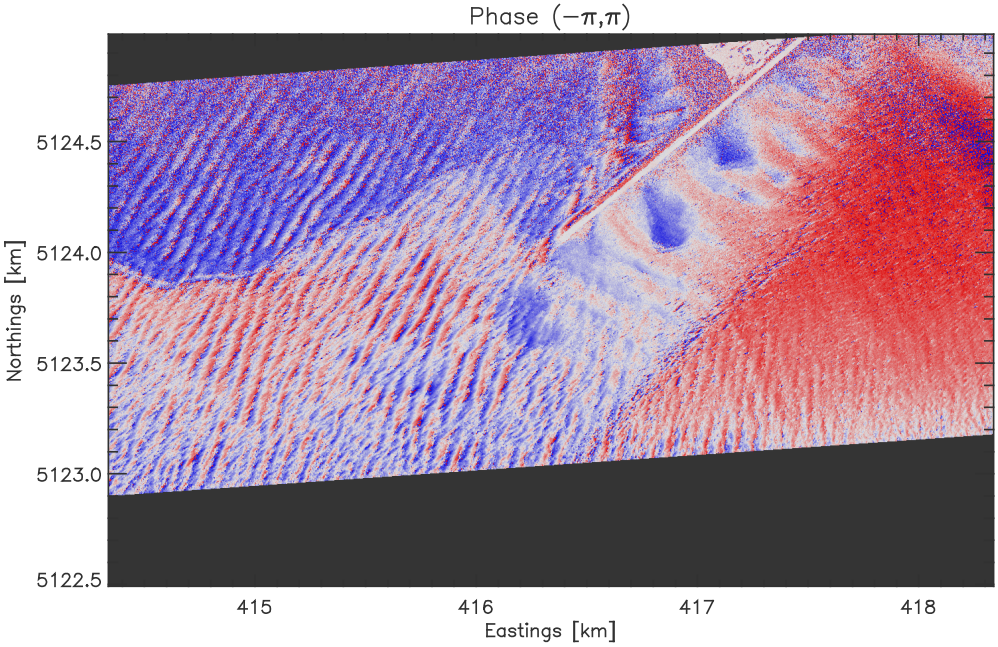

Figure C5: Interferometric phase image of the area around the North Jetty (top-left zone in Figure C4). The jetty is the solid white feature. Color is roughly proportional to line of sight component of velocity. The line of sight direction is roughly towards NNW. Blue is motion towards the radar, and red is motion away from the radar. The image was acquired on June 3, 2013 between 20:55:50 UTC and 21:02:32 UTC. The max ebb current was predicted to be 2.2 knots at 20:55 UTC.

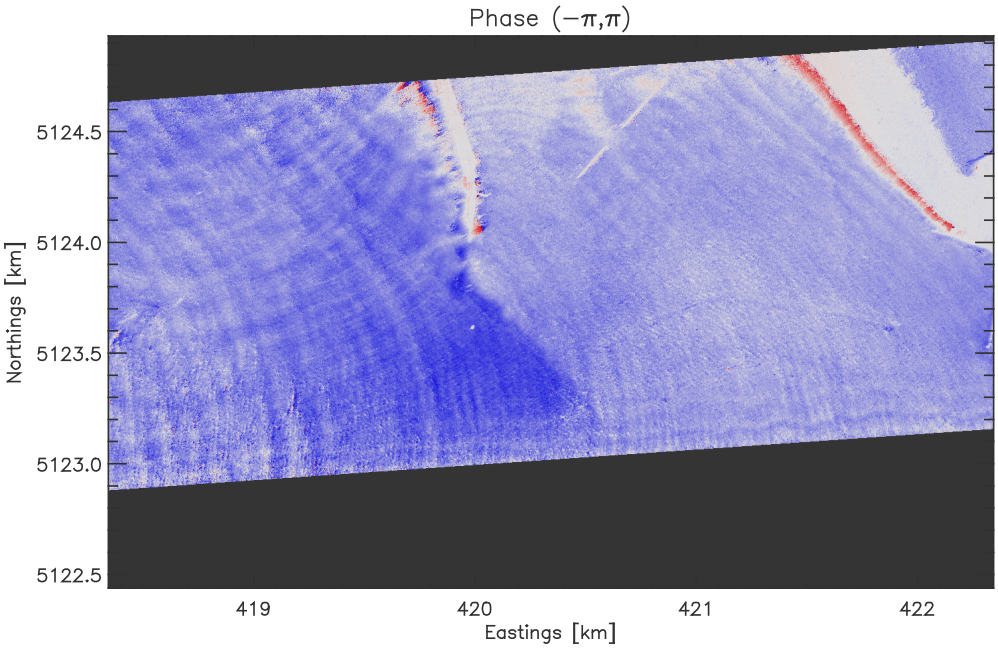

Figure C6: Interferometric phase image of the area around Jetty A (top-right zone in Figure C4). Color is roughly proportional to line of sight component of velocity. The line of sight direction is roughly towards NNW. Jetty A is the solid white structure at $x = 420$. Blue is motion towards the radar and red is away from the radar. The image was acquired on June 8, 2013 between 18:51:50 UTC and 18:58:03 UTC. The max flood current was predicted to be 3.1 knots at 19:55 UTC.

Some examples of interesting surface features in the hydrodynamics are strong streaks in the velocity field east of the North Jetty (Figure C5) during ebb, and changes in the wave spectrum on either side of fronts (Figure C5). Around Jetty A, we observe dramatic change in surface velocity signature (Figure C6). Rocky Geyer has suggested that he sees evidence in his data of a hydraulic jump around Jetty A. We also obverse the signature of a soliton wave east of Jetty A ($x = 421, y = 5123.6$). West of the mouth, the orbital velocity of the waves are large enough to clearly modulate the surface velocity field. A challenge for surface current retrieval with the MCR data will be to remove the wave field effects from the surface velocity measurements. We anticipate working with Roland Romeiser at the University of Miami on this problem.

Photographs of the Mouth of the Columbia River were taken during all flights with a hand-held camera. We are posting these photographs to a publicly available site for general use (http://apluwmcrphotos.shutterfly.com/pictures).

D. MICROWAVE REMOTE SENSING - OSU

During the past year we have continued to analyze data from both the New River Inlet experiment and the Duck Pilot. The Duck Pilot data was used for analysis of rip currents (in press Haller et al., *JWPCOE*) and also incorporated into the data assimilation modeling of Wilson et al. (submitted to *JGR*, 2013). We are also pursuing a comprehensive evaluation of the C-bathy depth estimation algorithm using our radar data from all three of the DARLA experiments with a comparison to ARGUS-derived bathymetry and ground truth. The purpose there is to quantify how bathymetric estimates from both sensors can best be fused and also to identify better error estimates for each product and the distribution of these errors in space. An additional purpose is to estimate the spatially-variable currents at high spatial resolution.

The third DARLA experiment took place at the Mouth of the Columbia River during May-June 2013. In May we established a radar observing site at the Cape Disappointment Coast Guard Station. This site is ~45m above MWL and offers an excellent vantage point for radar observing. We have permission to operate from this site until June 2014 and intend to collect observations continually during this period. Our analysis thus far has concentrated on two types of observations: 1) wave observations and 2) wave-averaged observations of tidal current features.

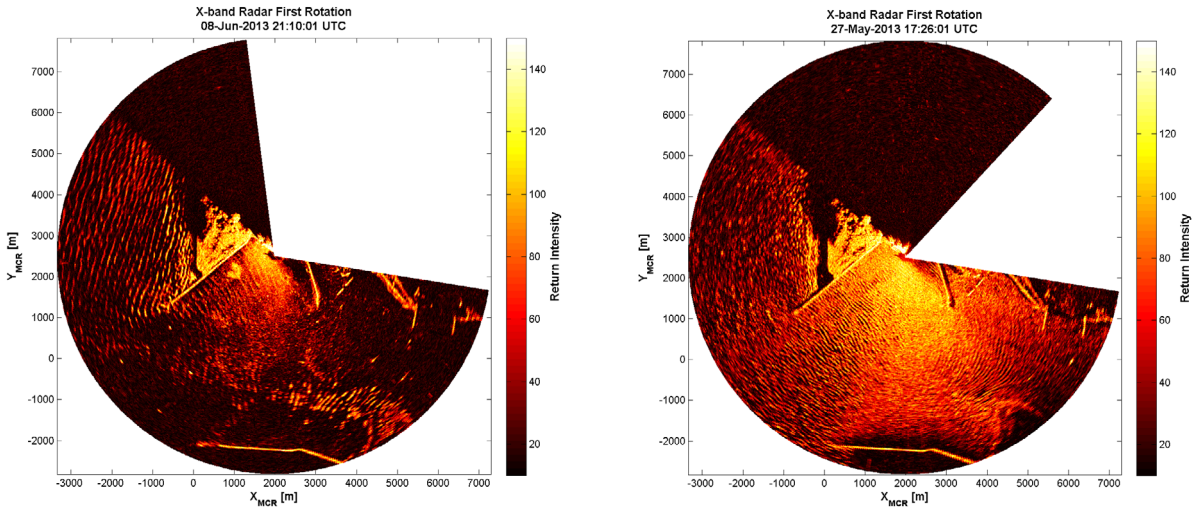

Figure D1: Radar snapshots under different wave conditions, (left) Hs=2m, Tp=14sec, (right) Hs=3.7m, Tp=8sec.

Figure D1 shows examples of two radar snapshots being used for wave analysis. In the left panel, long crested swell (Hs = 2 m; T = 14 s) arrives from WNW during flood. Once inside the jetties, some waves refract north into Middle Grounds while others continue on a straight course, breaking on Clatsop Spit. In the right panel, steep, energetic waves are incident from SW (Hs = 3.7 m; T = 8 s) near slack tide. These waves propagate toward Jetty A and turn southward, continuing down the river channel.

Full radar image sequences consist of 1024 or 2048 of these radar snapshots and can be used to estimate wavenumber vectors and the bathymetry using the C-bathy algorithm. Figure D2 shows an example bathymetric estimate (colors) and the estimated wavenumber vectors are overlaid. The wavenumber vectors and bathymetry are estimated at a spatial resolution of 50 m x 50 m. These estimates represent a temporal mean over a 12 hour period. The resolution is sufficient to resolve a break in the surf zone terrace along Benson Beach (x=0 m, y=2500 m), while identifying large-scale features such as the 25 m hole along the shipping channel (x= -800 m, y=200 m).

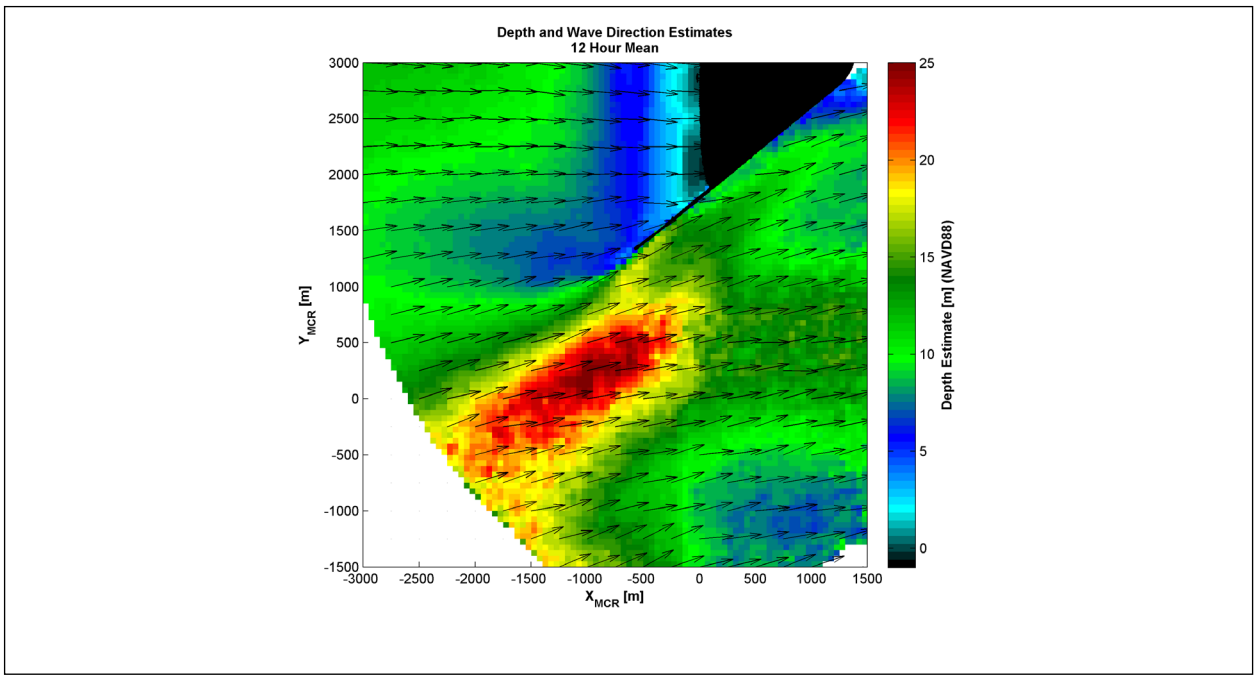

Figure D2:Wavenumber vectors and mean bathymetric estimate derived from 12 hours of marine radar data. Data are produced at 50 m x 50 m resolution but downsampled for plotting clarity.

By applying a lowpass filter to the radar image sequences we can isolate the signal at longer time scales (>1 minute). At the MCR, the low frequency image content is very rich. Example snapshots from the lowpass filtered image sequences are shown in Figure D3. The upper left panel shows three major fronts as ebb begins (A-C). Surface roughness manifestations of what may be shear instabilities are seen downstream of Jetty A at this time (D). An internal train approaching from the NW was imaged as ebb currents approached a maximum (lower left panel, E) and the north lateral plume front detached from the North Jetty (F). By the end of ebb, a strong anti-cyclonic circulation cell develops within Middle Grounds, resulting in a sharp front at the east end of the eddy (G). A surface roughness feature aligned parallel to the north jetty was observed to propagate toward the jetty (H) and subsequently reflect from the jetty (I). The feature has a period structure along its length with a length scale of 100-500 m. This feature appears during most ebbs, its origin is still not understood. Our ongoing analysis involves applying tracking algorithms to these features in order to quantify their speed of propagation and relationship to winds and tidal stage.

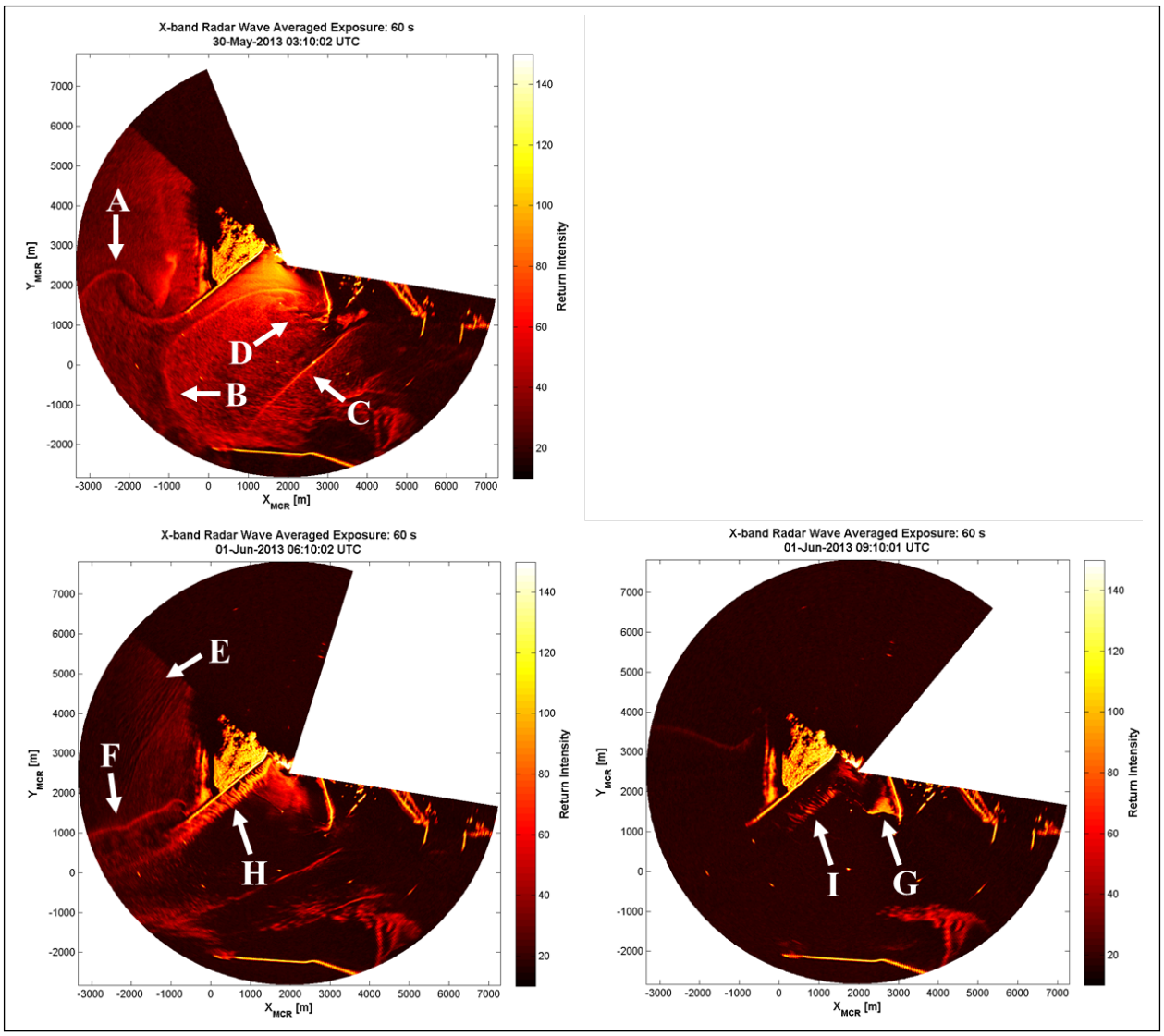

Figure D3:Lowpass filtered image snapshots isolate motions longer than 1 minute, (upper left) three major fronts (A-C) appear as ebb tide begins, (lower left) an internal wave train is visible (E) as ebb reaches maximum, (lower right) end of ebb tide, anti-cyclonic eddy in Middle Grounds produces a sharp front at the tip of Jetty A (G).

E. IN SITU MEASUREMENTS - UW

SWIFT drifter measurements were collected during a 2013 field effort at the Mouth of the Columbia River. Over 250 drifter missions were completed, over 36 days spanning April to September. Drifts were coordinated with the aircraft overflights, providing groundtruth measurements of: surface currents, waves, winds, turbulence, temperature, and salinity. The SWIFT drifter releases were staggered to obtain maximum coverage over synoptic time scales. SWIFT missions were coordinated with other drifters during overlap with the RIVET II effort in May and June. SWIFTs were modified for the MCR effort to include downlooking velocity profiles and surface salinity.

Figure E1 shows a common result from an ebb deployment of SWIFTs inside the river mouth. The drifters traverse 10-30 km offshore within a few hours, and the wave heights measured over the bar are

two to three times greater than the offshore values. Tracks from other days arc southwards, such that the total 250 tracks collected cover the entire region. The observation of increased wave height over the bar is consistent amoung all of the tracks. This wave shoaling is a result of both shallow depth and opposing currents, which slow the wave propagation and thus increase the wave height. This leads to oversteepening and breaking, which leads to turbulence.

Figure E1. Example SWIFT drifter measurements from 25 May 2013 at the Mouth of the Columbia River. Points are colored by wave height, ranging from 0 to 5 m, and there is strong wave intensification just offshore of the river mouth.

Figure E2 shows the along-track profile of wave breaking conditions and turbulence from the same example. Wave breaking occurs over the bar (x ~ 5 km) and offshore at the plume front (x ~ 30 km). The breaking is associated with high turbulent dissipate rates near the surface ($0.5 < z < 0$ m). Coincident with the breaking is strong turbulence at the interface between the fresh and salt water, especially where the plume "lifts off" from the bottom (x ~ 10 km). Upcoming data analysis will relate these turbulent signals to remote sensing data, such that both wave and plume dynamics can be mapped throughout the region. Data analysis will also address the possibility for wave breaking to provide an additional source of mixing to the river plume.

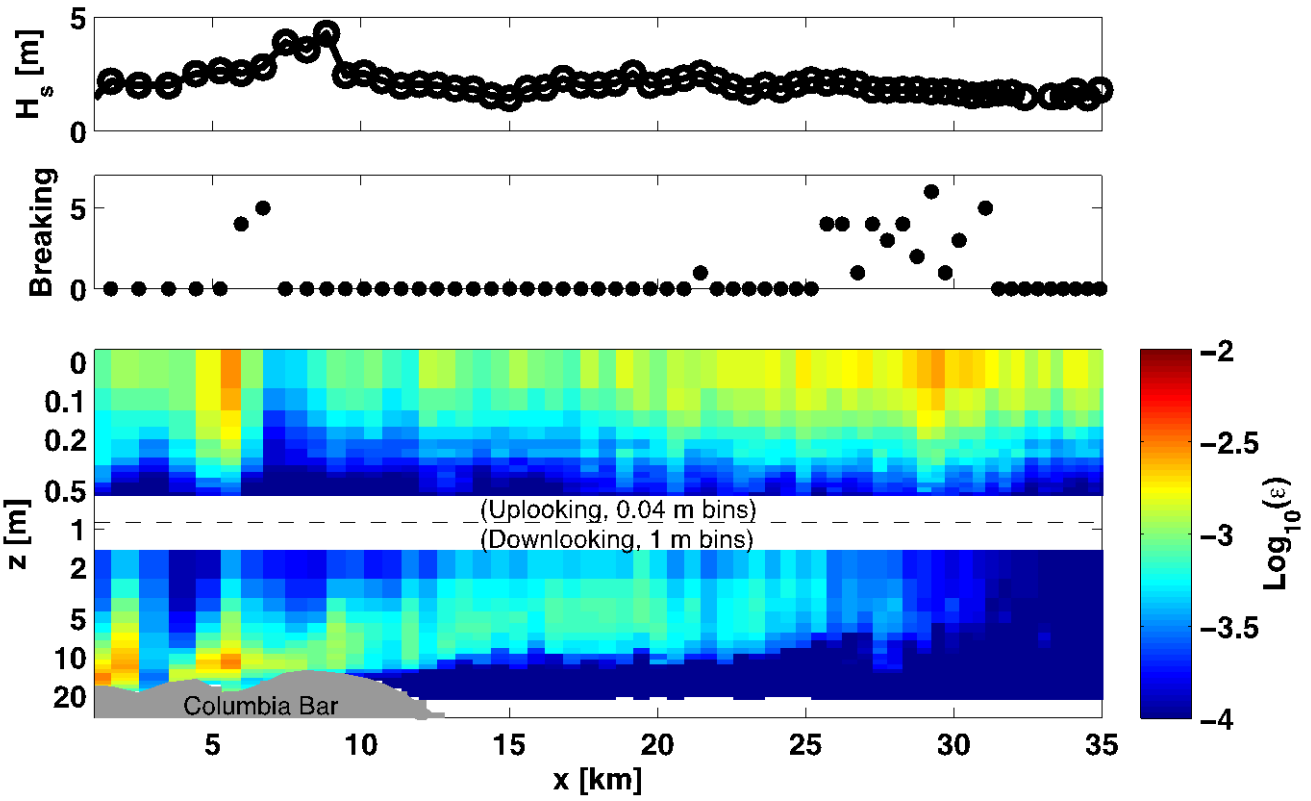

Figure E2. Along-track SWIFT measurements of: wave height, breaker count (per 5 minutes), near-surface turbulent dissipation rate, and full depth profile turbulent dissipation rate. Surface turbulence is well correlated with wave breaking, where as the full depth profile turbulence appears tied to the river plume (and interface with saltwater).

In addition to collecting new data at the MCR, data analysis from the previous field experiment at New River Inlet (NRI, 2012) has continued. This data analysis has successfully isolated the wave breaking mechanisms of depth shoaling, opposing currents, and wind forcing. The scales of associated turbulence are now being investigated, and the preliminary result is a preferrential scale for waves breaking against a current. The measurements at MCR (wave heights up to 6 m) are a unique extension of the dynamic range in the NRI data (wave heights up to 2.5 m). In fact, the MCR SWIFT data are the largest known sea state for measurements of wave breaking and plume turbulence. These observations were only possible using an autonmous platform, because research vessels could not transit the bar during rough conditions.

F. IN SITU MEASUREMENTS – WHOI

The data from wave and current sensors deployed at 32 locations near New River Inlet from April 27 through June 1, 2012 have undergone extensive quality control and have been placed on the WWW for use by other ONR team members and colleagues. The observations are being used as ground truth for remote sensing studies (e.g., Figure F1), and to initialize and test models that invert for the underlying bathymetry.

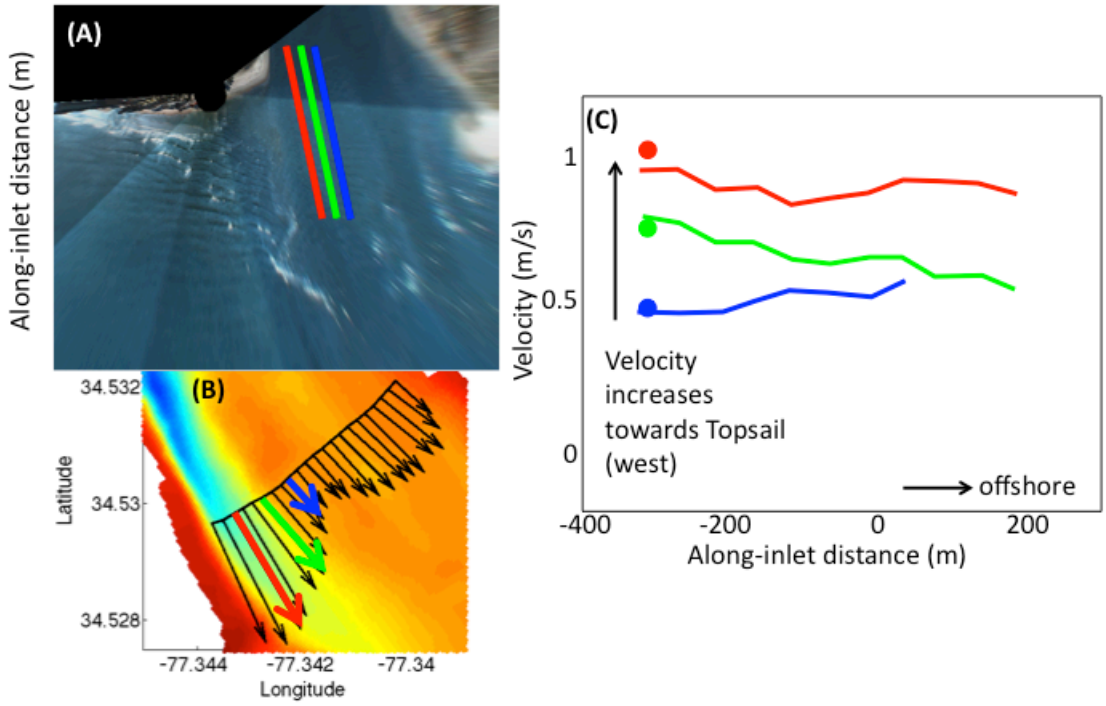

Figure F1. (A) Aerial view of the mouth of New River Inlet showing the 3 transect locations (colored lines: red near Topsail Beach, green on the northwestern edge of the main channel, and blue on the shoals to the northwest) of video-based estimates [Rob Holman] of surface flows. (B) Plan view of the bathymetry [Jesse McNinch] (color contours, red is 1 m depth, dark blue is 10 m depth) and near surface flows measured with a current profiler mounted on a boat (black arrows, largest is about 1 m/s) and estimated with video (colored arrows) over the same region and at the same time as the image in (A). (C) Velocity estimated from the video analysis (curves) and the current profiler (circles) versus along-inlet distance for the 3 transects shown in (A). [Video-based estimates of surface flows agree well with measurements from a boat-mounted current profiler. The ebb flows increase from the shoals across the main channel, and are strongest near Topsail Beach.]

Preliminary comparisons show that video-based estimates of along-inlet surface flows are consistent with measurements from a boat-mounted current profiler, and indicate that ebb velocities are strongest near Topsail Beach (on the southeast side of the inlet mouth) (Figure F1). In contrast, during flood flows, the profiler measurements show that currents are weakest near Topsail Beach, especially near the surface (not shown). Radar data suggest these weak flows are owing to an eddy that forms just inside the inlet mouth. Wave spectra estimated from SWIFT drifters [Jim Thomson] agree well with those based on data from *in situ* sensors, and show rapid dissipation of waves across the ebb shoal during ebb flows (not shown).

G. NUMERICAL MODELING AND DATA ASSIMILATION – OSU

During the past fiscal year, we have worked towards bathymetry estimation at two distinct sites – New River Inlet (NRI) and the Mouth of the Columbia River (MCR). Our efforts have primarily focused on employing ensemble-based data assimilation methodologies using only remotely sensed information. This methodology had previously been applied to bathymetry inversion in three settings: surf zone flows observed using in situ observations, river flows using drifter observations, and surf zone flows

observed with only remote sensors. The challenge then was to apply the method to the setting of a tidal inlet where both waves and current are important (and interact) and can be observed with remote sensing methodologies.

At NRI, we first conducted idealized twin-experiments where the "data" are derived from a model run over the measured ("true") bathymetry. The resulting waves and currents are then sampled at a resolution that matches the expected remotely sensed observations, resulting in a synthetic data set. We can then assimilate this synthetic data and ascertain if our method enables us to invert the system for bathymetry in this controlled setting. These twin-experiments help us isolate the information provided by each data type (e.g. currents vs waves, ebb observations versus flood observations) and pinpoint data requirements in a setting where the model physics completely describe the dynamics sampled by the synthetic data. In general, success in a twin-experiment does not guarantee success with actual observations, but is a pre-requisite to success.

The twin experiments were successful and led us to isolate three primary data types for depth inversion efforts using actual observations at NRI. In particular, the focus is primarily on surface current observations using SAR images and wavenumber information (at a given frequency) derived from X-band radar observations. Note that the former provides high-quality observations inside and near the inlet mouth, whereas the latter covers a region outside of the inlet mouth (on the shoals) and is not as useful inside the inlet where surface waves do not penetrate. Surface current observations from drifters (e.g. SWIFT) are also utilized and prove useful to further constrain the system.

Results from simulations during ebb conditions on May 10 are shown in Figure G1. Our prior estimate of bathymetry is based on a nearly along-channel uniform river bathymetry paired with a generic inlet and beach. Assimilation of SAR, X-band radar and drifter observations improve the bathymetry estimate significantly and indicate that the method can successfully predict locations of major bathymetric features (e.g. shoals and pools) that were not part of the prior estimate.

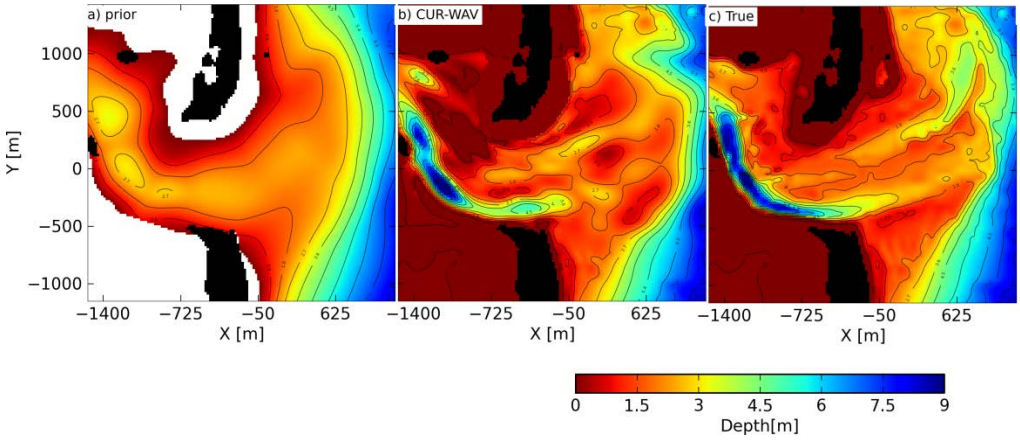

Figure G1: a) Prior bathymetry estimate, b) posterior bathymetry estimate after assimilation of current and wave information from three data sources for May 10, c) true measured bathymetry. The depth inversion method is capable of estimating the locations and depth of major bathymetric features (e.g. shoals and deep pools) that were not present in the prior estimate.

The twin-experiments indicate that assimilation of flood currents may provide additional information about the deep river channel. This information is apparently not contained in the data during ebb conditions because the ebb currents are less sensitive to the bathymetry in that area. Further, the twin experiments indicate that an iterative process (adopting the posterior bathymetry as the new prior and going through the assimilation exercise again) can result in improved estimates. This is because the method essentially relies on a linearization around the prior bathymetry estimate and large corrections cannot be accommodated. The iterative process allows for the update of the prior estimate and hence overcomes this shortcoming. Incorporating these two improvements into the scheme involving NRI observations is underway. We are also working on assimilating additional data types (e.g. velocities derived from IR, dissipation estimates derived from EO and other sensors).

Further analysis for NRI has includes the isolation of wave-current interaction processes. In particular, we have examined the effect of wave forcing near the inlet mouth and its potential of altering the tidal circulation. This is a feedback process that is often neglected at such sites; even if the effect of the currents on the waves is considered, the effect of the waves on the currents is often not modeled. When this feedback is included, we find that the circulation is affected both quantitatively and qualitatively (see Figure G2). Essentially, the effect of wave breaking over the shoals just outside the inlet generates shoreward-directed wave forcing that results in a significant modification to the tidal velocities. During ebb conditions, the ebb jet is diverted into the deeper channels, and much vorticity activity results. During flood conditions (not shown), the current magnitude into the inlet is increased and the wave forcing enables further water mass to be pumped into the inlet. We are further pursuing work on isolating and analyzing these effects to further our understanding of when the feedback between wave motion and circulation should not be neglected.

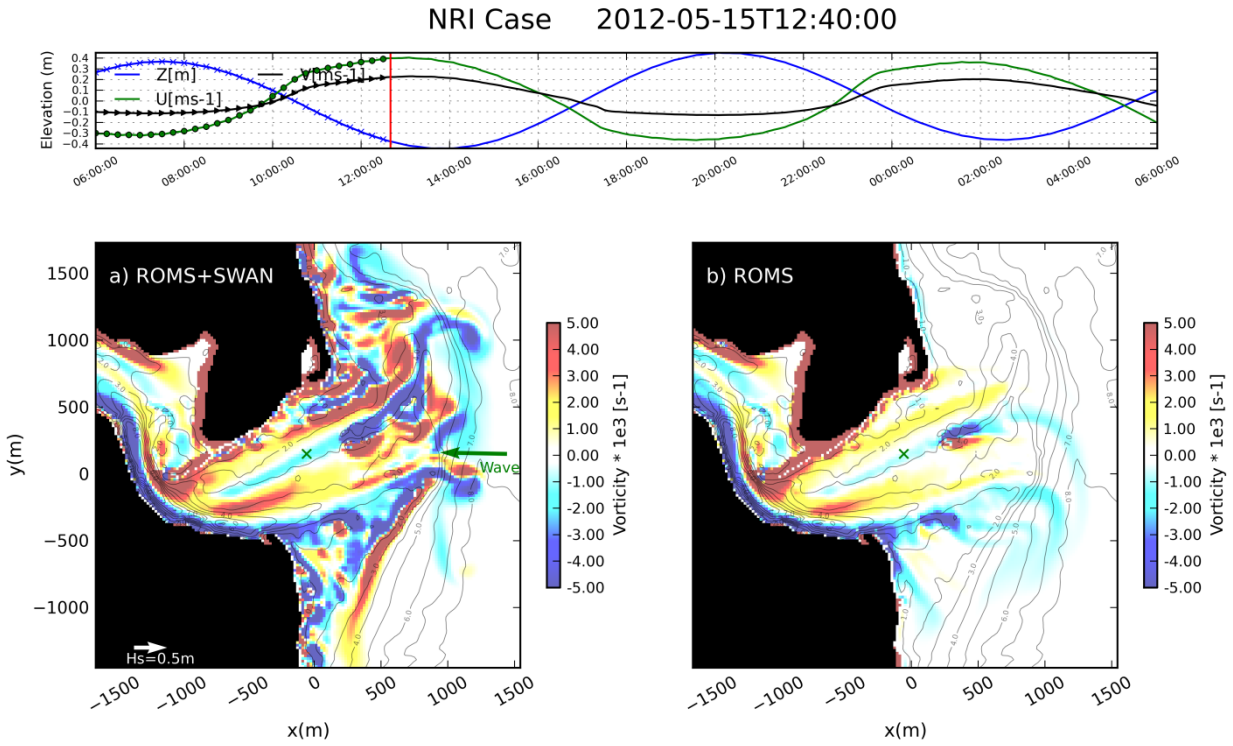

Figure G2: Time series of currents and surface elevation (upper panel), vorticity resulting from a fully-coupled wave-circulation simulation (lower left panel) and a circulation-only simulation (lower right panel). The snapshots in the lower panels are at the time indicated by the red line in the upper time series plot and correspond to ebb conditions. The results indicate qualitative and quantitative changes to the circulation due to the effects of wave breaking on the shoals outside of the inlet.

Finally, we have been making progress on applying the developed methodology at the Mouth of the Columbia River (MCR), where similar types of observations are now avaialble. Our first efforts focussed on calibrating our coupeld SWAN+ROMS simulations using observations from a previous field effort at the MCR (the Mega-transect experiment). Of special interest are the effects of wave-current interaction and their implications in this setting where the water depth outide of the inlet is much deeper (compared to NRI) and no depth-induced wave breaking is expected in near the mouth. However, the tidal currents are much stronger here, and current-induced wave breaking is a possibility, and the effects of the wave forcing resulting from such wave breaking may also have the potential of modifying the circulation.

Our initial simulations indicate that the effect of the strong tidal currents on the waves is significant, potentially doubling the wave height near the mouth and introducing a distinct tidal signal in the wave height times series. In this setting the effect of the waves on the tidal circulation is more minor, primarily because the tidal currents are very strong and the wave effect is not large enough to make signifcant qualitative changes to the circulation. Further work will involve further model validation and the application of the depth inversion methodology to this setting.

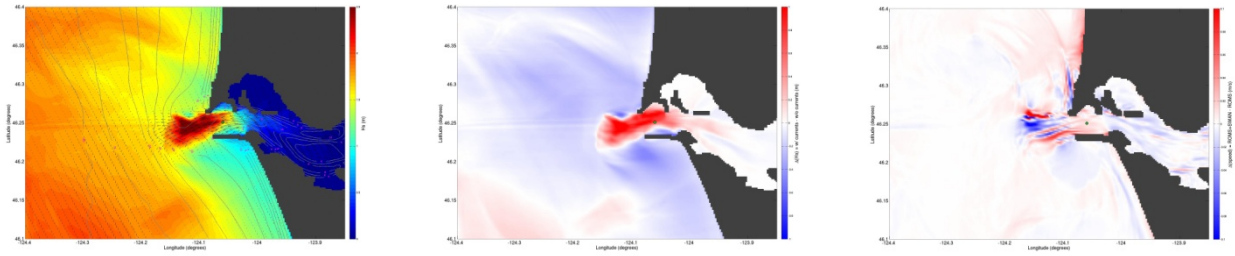

Figure G3: Wave height and circulation for a fully coupled model run during ebb conditions (left panel). The changes in the wave height induced by the presence of the ebb currents (middle panel), and the changes in the circulation induced by the effect of the waves (right panel) are also shown.

IMPACT/APPLICATIONS

Our results demonstrate how currently available prediction schemes and remote sensing observing systems can be combined for operational applications. Use of a miniaturized airborne along-track-interferometic SAR to measure surface velocities provides a new and powerful tool for area-extensive measurements in the field. The development of cBathy has high impact in finally allowing robust estimation of bathymetry with reasonable accuracy based only on continuing optical (or radar or IR) sampling. Bathymetry has always been an expensive and very rare variable to measure and one whose absence destroys the credibility of numerical model predictions.

RELATED PROJECTS

The DARLA MURI effort is closely related to the ongoing ONR RIVET DRI through participation in field campaigns. This work complements the traditional interests of NRL-SSC in littoral remote sensing including the LENS program and continuations thereof and efforts to carry out nearshore prediction based on UAV sensor inputs. This work also complements recent Oregon State efforts to greatly improve the utility and usability of UAV platforms for all purposes. The WHOI *in situ* wave and current observations near New River Inlet were collected as part of a DRI, and are being used to develop, test, and improve models for wave propagation, circulation, and morphological evolution, as well as to ground truth remote sensing observations.

PUBLICATIONS

Catalán, P.A., M.C. Haller, and W.J. Plant, Microwave backscattering from surf zone waves, *J. Geophys. Res.*, 2012.

Holman, R.A. and M.C. Haller, Nearshore remote sensing, *Annual Review of Marine Science*, to appear in Volume 5, January 2013. [in press]

Holman, R.A., Plant, N.G. and K.T. Holland, cBathy: A robust algorithm for estimating nearshore bathymetry, *J. Geophys. Res*., 2012.

Thomson, J., Observations of wave breaking dissipation from a SWIFT drifter, *J. Atmos. & Ocean. Tech.,* 2012. [in press]